An efficient aircraft conflict probability estimation method using a spatial multi-resolution scheme

Seyedhamed Seyedipour, Hadi Nobahari, Maria Prandini

***Abstract*— In this paper, we propose an improved variant of an aircraft conflict probability estimation method recently introduced in the literature. The key innovative aspect consists in the adoption of an inner and outer block cover of the conflict zone that is tuned to the local conflict probability estimation error, thus resulting in a spatial multi-resolution scheme. As in the original method, an estimate of the conflict probability with accuracy guarantees is provided.**

Simulation results show that the proposed method is more efficient than the original one, in that it provides a coverage of the conflict zone for conflict probability estimation that is adapted to the probability distribution of the aircraft relative distance. Computational time is then smaller because of the lower number of blocks needed for the inner and outer covers of the conflict zone.

I. INTRODUCTION

Safety in an air traffic management system (ATMS) is maintained by monitoring the trajectories of aircraft to prevent them getting closer than a predefined safe distance. This situation is called conflict and when a conflict is predicted, aircraft trajectories are changed to avoid its actual occurrence. This task is performed by air traffic controllers (ATCs) on a mid-term time scale of 10 to 20 minutes.

ATMS is facing a constant growth in air transportation [1], which is causing an increase of the ATCs workload. Free flight demand and the integration of unmanned aerial vehicles into civil airspace [2], [3] are further challenging ATMSs. Such challenges prompt the need for a modernization of the current ATMS structure. A key goal of ATMS modernization is increasing safety. A promising approach to increase safety in future airspace is to develop methods that perform conflict detection (CD) in a more scalable, flexible, and automated way.

CD methods are divided into nominal, worst-case, and probabilistic methods [4]. In the nominal method, the reference trajectories of the two aircraft are considered to predict if the distance of two aircraft will get smaller than the safety value. In the worst-case approach, all possible trajectory realizations are considered and a conflict is detected if the safety threshold is violated by any of the admissible trajectories. The probabilistic method resorts to a stochastic characterization of the aircraft relative distance and compute the conflict probability as a measure of the likelihood that a conflict occurs, thus avoiding the conservativeness of the worst-case approach.

In this paper, we propose a new method for conflict probability estimation that is useful for mid-term probabilistic CD. The method is inspired by [5] where conflict probability for two-aircraft encounters is estimated with deterministic accuracy bounds by using an inner and outer block coverage of the conflict zone. The present work further improves the performance of the method in [5], while retaining the accuracy bounds. This is achieved by implementing a spatial multi-resolution scheme where the blocks covers are tuned to the relative aircraft distance probability distribution while imposing a desired accuracy level on the conflict probability estimate.

The remainder of this paper is structured as follows. Section II presents a short review of the probabilistic CD methods that are relevant to the present work. Section III describes the adopted aircraft and wind model. Section IV formulates the conflict probability estimation problem. The proposed method is introduced in Section V. Finally, numerical results and conclusion are presented in Sections VI and VII, respectively.

II. REVIEW OF RELEVANT PROBABILISTIC CONFLICT DETECTION METHODS

Probabilistic CD methods can be classified as randomized methods, where the conflict probability or related quantities are estimated via simulation-based methods, [6]–[10], and approximate methods, where a set of approximations and/or suitable transformations are performed to compute the conflict probability relying on its analytic expression, [5], [11]–[20]. The approach in this paper belongs to the latter category.

In [11], [12], an algebraic approximation of a quadratic form of the relative aircraft distance $\Delta\mathbf{r}$ is adopted to compute the conflict probability, using a linear model subject to Gaussian uncertainty in two-dimensional (2D) encounters. The quality of the approximation can be improved by increasing the number of terms of a Laurent series expansion. In [13] and [14] the probability density function (pdf) of $\Delta\mathbf{r}$ is computed at the minimum distance in 2D encounters. Then, the conflict probability is computed by integrating the obtained pdf. In [13] only one-leg trajectories are studied, whereas in [14] multi-leg trajectories are considered. No accuracy of the obtained estimate is provided in [11]–[14].

A method to compute the conflict probability for a 2D linear model is proposed in [15]. In this method, risk is obtained by integrating the conflicted part of the pdf of $\Delta\mathbf{r}$.

Seyedhamed Seyedipour and Hadi Nobahari are with the Department of Aerospace Engineering, Sharif University of Technology, Tehran, Iran, email: seyedipour_seyedhamed@ae.sharif.edu, nobahari@sharif.edu

Maria Prandini is with the Dipartimento di Elettronica Informazione e Bioingegneria, Politecnico di Milano, Piazza Leonardo da Vinci 32, 20133 Milano, Italy, email: maria.prandini@polimi.it

Then, sum of the risks computed along a reference time interval is taken as an estimate of the conflict probability, which involves propagating at every time step the part of the pdf of $\Delta\mathbf{r}$ outside the conflict zone. Although the initial pdf is assumed to be Gaussian, the propagated pdf does not remain Gaussian. Hence, this process requires propagation of a distorted pdf which is complicated.

A method called probability flow is proposed in [16]. In this method, the rate of probability entering/exiting the conflict zone is calculated and then integrated to compute the conflict probability, based on a three-dimensional linear model subject to Gaussian uncertainty. A reformulation of the probability flow method is studied in [17]. In all formulations, the method provides inaccurate estimates for long conflict scenarios [21], and no accuracy bound is provided.

In the seminal work in [18], the relative aircraft distance $\Delta\mathbf{r}$ in 2D en-route airspace is modeled as a 2D Gaussian variable and a coordinate transformation is adopted so that its covariance matrix becomes the identity matrix and the two Gaussian components independent. This transformation reshapes the conflict zone in 2D en-route airspace from a circle to an ellipse, which is then extended over one of the space axes under constant relative heading and velocity assumptions, to the purpose of estimating the maximum conflict probability in encounters. In the case when the relative heading and velocity are not constant, reference is made to the minimum distance configuration. Inspired by [18], in [19] an upper bound on the instantaneous conflict probability for a 2D linear Gaussian model of the relative distance is computed by rotating the (transformed) ellipsoidal conflict zone so that its axes are aligned with the coordinate axes. The ellipse is then over-approximated via two appropriately chosen blocks, which ease the estimation of an upper bound on the instantaneous conflict probability via integration of the 2D Gaussian pdf. By using a multi-block cover of the ellipsoidal conflict zone, a more accurate over-approximation of the instantaneous conflict probability is determined in [20]. In both [19] and [20], no accuracy bound is provided. In [5], the use of an inner and an outer multi-block cover of the ellipsoidal conflict zone allows to calculate both an upper and a lower bound of the instantaneous conflict probability, from which estimate and accuracy are derived. Accuracy is then adjusted by increasing the number of blocks according to a uniform coverage strategy.

In this paper, we propose a variant of [5] where the ellipsoidal conflict zone is approximated in a more efficient way, through a strategy tuned to the relative distance probability distribution. The new approximation method implements a spatial multi-resolution scheme for both the inner and the outer covers, which allows to provide an accuracy bound on the instantaneous conflict probability estimate as in [5].

III. AIRCRAFT AND WIND MODEL

We consider aircraft flying at the same constant altitude and use the following 2D version of the aircraft and wind model presented in [22]:

$$\begin{cases} \dot{x} = v\cos\psi + w_x \\ \dot{y} = v\sin\psi + w_y \\ \dot{\psi} = \frac{L\sin\phi_c}{mv} \\ \dot{m} = -\gamma T \end{cases} \tag{1}$$

Vector $\mathbf{r} = [x\ y]^\top$ denotes the aircraft position in the inertial frame, ψ and m are aircraft heading angle and mass, respectively. Moreover, γ, T, L, ϕ_c, and v are fuel consumption rate, thrust, lift, commanded bank angle, and air speed, respectively. The terms w_x and w_y are the components along the x and y axes of the inertial frame that are sampled from the spatially and temporally correlated Gaussian wind field model described in [22], [23]. The mass and nominal trajectory of aircraft are assumed to be known. At each simulation time, ϕ_c is calculated so that the aircraft follows its flight-plan path, defined by a sequence of way-points (see [22] for more details).

IV. CONFLICT PROBABILITY ESTIMATION PROBLEM

Consider two aircraft, A and B, traveling at the same constant altitude with air speed v_A and v_B, respectively. The position vectors of two aircraft can be expressed as

$$\begin{cases} \mathbf{r}_A = \bar{\mathbf{r}}_A + \tilde{\mathbf{r}}_A \\ \mathbf{r}_B = \bar{\mathbf{r}}_B + \tilde{\mathbf{r}}_B \end{cases},$$

where $\bar{\mathbf{r}}$ and $\tilde{\mathbf{r}}$ denotes the nominal and stochastic part of the $\mathbf{r}$. The relative position of the two aircraft can then be written as

$$\Delta\mathbf{r} = \Delta\bar{\mathbf{r}} + \Delta\tilde{\mathbf{r}}$$

where $\Delta\bar{\mathbf{r}} = \bar{\mathbf{r}}_A - \bar{\mathbf{r}}_B$ and $\Delta\tilde{\mathbf{r}} = \tilde{\mathbf{r}}_A - \tilde{\mathbf{r}}_B$. The covariance matrix of $\Delta\mathbf{r}$ is finally given by

$$\begin{aligned} \mathbf{V} = \mathrm{E}[\Delta\mathbf{r}\Delta\mathbf{r}^\top] = \mathrm{E}[\tilde{\mathbf{r}}_A\tilde{\mathbf{r}}_A^\top] + \mathrm{E}[\tilde{\mathbf{r}}_B\tilde{\mathbf{r}}_B^\top] \\ -\mathrm{E}[\tilde{\mathbf{r}}_A\tilde{\mathbf{r}}_B^\top] - \mathrm{E}[\tilde{\mathbf{r}}_B\tilde{\mathbf{r}}_A^\top] \end{aligned} \tag{2}$$

Note that $\mathrm{E}[\tilde{\mathbf{r}}_A\tilde{\mathbf{r}}_B^\top]$ and $\mathrm{E}[\tilde{\mathbf{r}}_B\tilde{\mathbf{r}}_A^\top]$ are cross-correlation terms that can be computed through Monte Carlo simulations (see [22]). These terms are usually assumed to be zero, which is however a reasonable assumption only when aircraft are far apart.

If the absolute value of the relative distance $\|\Delta\mathbf{r}\|$ is smaller than the safety distance, which is defined by regulations as $\mathrm{S_c} = 5$ nmi in en-route airspace, then a conflict occurs. Thus, conflict probability can be defined as

$$p_c = \int_D f(s)ds, \tag{3}$$

where f is the pdf of $\Delta\mathbf{r}$ and $\mathrm{D} = \{v \in \Re^2 : v^\top v \leq {\mathrm{S_c}}^2\}$ denotes the conflict zone that is a circular area centered at the origin with radius equal to $\mathrm{S_c}$.

The uncertainty which affects the aircraft can be assumed to be Gaussian [18], [23], [24]. Consequently, $\Delta\mathbf{r}$ is a 2D Gaussian random variable and eq. (3) can be rewritten

$$p_c = \int_D G_2(s; \Delta\bar{\mathbf{r}}, \mathbf{V})ds, \tag{4}$$

where G_2 denotes a 2D Gaussian pdf.

As the components of $\Delta\mathbf{r}$ are dependent and the domain of integration is circular, the integral in eq. (4) is hard to compute. In the next section we describe the proposed method to approximate such an integral.

V. PROPOSED CONFLICT PROBABILITY ESTIMATION METHOD

This section presents the proposed conflict probability estimation method. As explained in Section II, space coordinate transformation is a commonly adopted idea to compute the conflict probability. This transformation is obtained by applying Cholesky decomposition to the covariance matrix $\mathbf{V = LL}^\top$, and setting $\mathbf{T} = \mathbf{L}^{-1}$. The transformed conflict zone is an ellipse with an arbitrary orientation. A rotation matrix, $\mathbf{R}$, can then be employed to rotate it so as to obtain an ellipse D' with axes aligned with the coordinate axes, [25]. Finally, the new coordinate variables and the associated relative position covariance matrix are given by

$$\begin{bmatrix}\xi & \eta\end{bmatrix}^\top = \mathbf{RT}\begin{bmatrix}x & y\end{bmatrix}^\top, \mathbf{M = (RT)V(RT)}^\top = \mathbf{I},$$

where $\mathbf{I}$ denotes the 2D identity matrix. As a result, eq. (4) can be rewritten as [18], [19]

$$p_{\mathrm{c}} = \int_{\mathrm{D}'} G(\xi;\bar{\xi},1)G(\eta;\bar{\eta},1)d\xi d\eta, \tag{5}$$

where $[\bar{\xi}\ \bar{\eta}]^\top = \mathbf{RT}\Delta\bar{\mathbf{r}}$.

Eq. (5) entails that, if the integration domain were rectangular, then, the conflict probability could be determined by integrating each one-dimensional Gaussian pdf over the associated coordinate and then computing the product. The idea is then to estimate the conflict probability by approximating the ellipse with some blocks with dimensions parallel to the coordinate (ξ, η) axes. The process of computing the upper and lower bounds of the conflict probability and approximating the ellipse by a suitably chosen set of blocks is explained in Section V-A and V-B, respectively.

A. Upper and lower bounds of the conflict probability

Let us consider an inner and an outer block-cover of the ellipsoidal conflict zone, as shown in Figure 1. Denote the dimensions of the i-th block as $[\xi^{\mathrm{UB}}_{\mathrm{i,min}}, \xi^{\mathrm{UB}}_{\mathrm{i,max}}]$ and $[\eta^{\mathrm{UB}}_{\mathrm{i,min}}, \eta^{\mathrm{UB}}_{\mathrm{i,max}}] = [-\eta^{\mathrm{M}}_i, \eta^{\mathrm{M}}_i]$ for the outer cover and $[\xi^{\mathrm{LB}}_{\mathrm{i,min}}, \xi^{\mathrm{LB}}_{\mathrm{i,max}}]$ and $[\eta^{\mathrm{LB}}_{\mathrm{i,min}}, \eta^{\mathrm{LB}}_{\mathrm{i,max}}] = [-\eta^{\mathrm{m}}_i, \eta^{\mathrm{m}}_i]$ for the inner cover.

Consider the outer cover. An upper bound on the conflict probability for the i-th block can be computed as

$$p^{\mathrm{UB}}_{\mathrm{c},i} = \left(\Psi_{\bar{\eta}}(\eta^{\mathrm{M}}_i) - \Psi_{\bar{\eta}}(-\eta^{\mathrm{M}}_i)\right) \cdot \left(\Psi_{\bar{\xi}}(\xi^{\mathrm{UB}}_{\mathrm{i,max}}) - \Psi_{\bar{\xi}}(\xi^{\mathrm{UB}}_{\mathrm{i,min}})\right)$$

with $\Psi_\alpha(x) := \int_{-\infty}^{x} \mathcal{G}(v;\alpha,1)dv$ as cumulative distribution function of the standard normal Gaussian pdf. Similarly, a lower bound of the conflict probability for the i-th block can be computed as

$$p^{\mathrm{LB}}_{\mathrm{c},i} = \left(\Psi_{\bar{\eta}}(\eta^{\mathrm{m}}_i) - \Psi_{\bar{\eta}}(-\eta^{\mathrm{m}}_i)\right) \cdot \left(\Psi_{\bar{\xi}}(\xi^{\mathrm{LB}}_{\mathrm{i,max}}) - \Psi_{\bar{\xi}}(\xi^{\mathrm{LB}}_{\mathrm{i,min}})\right).$$

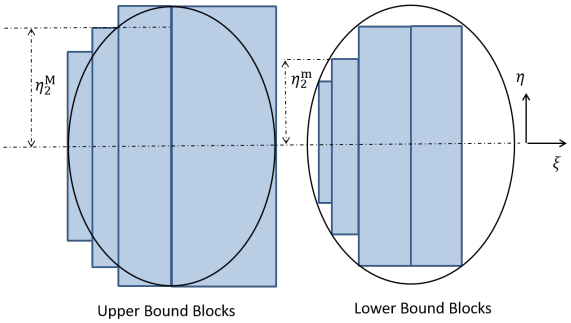

Fig. 1: Outer and inner covers of the conflict zone.

If we define the estimate of the conflict probability as

$$\hat{p}_{\mathrm{c},i} = \frac{p^{\mathrm{UB}}_{\mathrm{c},i} + p^{\mathrm{LB}}_{\mathrm{c},i}}{2} \tag{6}$$

and the estimation error as

$$\epsilon_i = \frac{p^{\mathrm{UB}}_{\mathrm{c},i} - p^{\mathrm{LB}}_{\mathrm{c},i}}{2} \tag{7}$$

The maximum conflict probability error over blocks is then given by

$$\epsilon_{\max} = \max_{i=1,2,..,N} \epsilon_i$$

The actual value of the probability of conflict $p_{\mathrm{c},i}$ satisfies

$$p_{\mathrm{c},i} \in (\hat{p}_{\mathrm{c},i} - \epsilon_i,\ \hat{p}_{\mathrm{c},i} + \epsilon_i).$$

Considering the total covers, the conflict probability is determined as

$$\hat{p}_{\mathrm{c}} = \sum_{i=1}^{\mathrm{N}} \hat{p}_{\mathrm{c},i} \tag{8}$$

and the error of the estimate can be computed as

$$\epsilon = \sum_{i=1}^{\mathrm{N}} \epsilon_i. \tag{9}$$

As a result, $\hat{p}_{\mathrm{c}} - \epsilon$ and $\hat{p}_{\mathrm{c}} + \epsilon$ represent a lower and an upper bounds on the conflict probability.

B. Multi-resolution algorithm

We now describe the proposed multi-resolution scheme to build the inner and outer covers of the ellipsoidal conflict zone.

The idea is as simple as follows. We start from a rough cover and keep dividing each block in two equal-width parts along the ξ axis as long as the conflict probability error computed over that block is larger than a predefined value. In this way, a refinement of the block-cover is performed not all-over the conflict zone (as it is done in [5] where a uniform space partitioning is considered on the ξ axis), but only locally, in those regions where the contribution to the overall estimation error is larger. This corresponds to repeatedly applying a binary partitioning.

Algorithm 1, called multi-resolution conflict probability computation (MR-CPC), performs the described recursive block partitioning. First, corresponding interval related to the upper bound and lower bound blocks are determined

(lines 5-13). Then, $\hat{p}_{\rm c}$ and ϵ are computed using eq. (6) and eq. (7) (line 14). If the desired accuracy $\epsilon_{\rm des}$ is not reached yet and number of iterations, D, is less than the maximum number of iterations, $D_{\max}$, then, the block is divided into two equal-width child blocks. Then, the process is iterated for each derived child block (lines 15-20). The final estimate and accuracy $\hat{p}_{\rm c}$ and ϵ are obtained by summing up the values of $\hat{p}_{\rm c}$ and ϵ obtained for the child blocks. Function $f_\eta(\xi)$ in Algorithm 1 computes the value of the η coordinate of the point in the ellipsoidal conflict zone that is in the positive η half-plane and has ξ coordinate.

Algorithm 1 MR-CPC

Input: $\xi_{\min}, \xi_{\max}, \eta_{\min}, \eta_{\max}, D, D_{\max}, \epsilon_{\rm des}$
Output: $\hat{p}_{\rm c}, \epsilon$
1: $\xi^{\rm UB}_{\min} = \xi_{\min}$ and $\xi^{\rm UB}_{\max} = \xi_{\max}$
2: **if** $D = 1$ **then**
3: $\quad \xi^{\rm UB}_{\min} = 0$
4: **end if**
5: calculate $\eta_1 = f_\eta(\xi^{\rm UB}_{\min})$ and $\eta_2 = f_\eta(\xi^{\rm UB}_{\max})$
6: $\eta^{\rm M} = \max(\eta_1, \eta_2)$ and $\eta^{\rm m} = \min(\eta_1, \eta_2)$
7: **if** $\eta^{\rm m} = 0$ **then**
8: $\quad \xi_{\rm mid} = |\frac{\xi_{\min}+\xi_{\max}}{2}|$
9: $\quad \eta^{\rm m} = f_\eta(\xi_{\rm mid})$
10: $\quad \xi^{\rm LB}_{\min} = \max(-\xi_{\rm mid}, \xi_{\min})$ and $\xi^{\rm LB}_{\max} = \min(\xi_{\rm mid}, \xi_{\max})$
11: **else**
12: $\quad \xi^{\rm LB}_{\min} = \xi_{\min}$ and $\xi^{\rm LB}_{\max} = \xi_{\max}$
13: **end if**
14: Compute $\hat{p}_{\rm c}$ and ϵ using equations (6) and (7)
15: **if** $\epsilon > \epsilon_{\rm des}$ and $D < D_{\max}$ **then**
16: $\quad \xi_{\rm mid} = \frac{\xi_{\min}+\xi_{\max}}{2}$
17: $\quad [\hat{p}_{\rm c,1}, \epsilon_1] =$ MR-CPC$(\xi_{\min}, \xi_{\rm mid}, \eta_{\min}, \eta_{\max}, D+1, D_{\max}, \epsilon_{\rm des})$
18: $\quad [\hat{p}_{\rm c,2}, \epsilon_2] =$ MR-CPC$(\xi_{\rm mid}, \xi_{\max}, \eta_{\min}, \eta_{\max}, D+1, D_{\max}, \epsilon_{\rm des})$
19: $\quad \hat{p}_{\rm c} = \hat{p}_{\rm c,1} + \hat{p}_{\rm c,2}$ and $\epsilon = \epsilon_1 + \epsilon_2$
20: **end if**

VI. NUMERICAL RESULTS

In this section, we compare the proposed MR-CPC method with those presented in [19], [20] and [5], which in the sequel will be referred to as I-CPC, MB-CPC and ULB-CPC methods (see Section II for a short description).

For comparative purposes, we estimate the conflict probability by running 1000 Monte Carlo simulations of the two-aircraft encounter, using a MATLAB version of the aircraft motion simulator described in [22] and [23], which includes a fully spatially and temporally correlated Gaussian wind field model. The simulator is also used to provide a Monte Carlo estimate of the covariance matrix of the aircraft relative distance, which is needed in each scenario to determine the conflict probability via I-CPC, MB-CPC, ULB-CPC and MR-CPC methods.

Recall that I-CPC approximates the conflict zone with two blocks, whereas MB-CPC and ULB-CPC can improve the conflict probability estimate by adding blocks to the conflict zone cover. However, only the ULB-CPC method can be used to automatically improve the accuracy as it provides accuracy bounds on the estimated conflict probability. This is done in Algorithm 2, where the conflict probability, the conflict probability error, and the maximum conflict probability error over blocks are estimated for a predefined number of blocks (line 2), and then, if the error is not satisfactory and the maximum number of blocks is not reached, the number of blocks is increased and estimates are again computed for the new block number (lines 3-6).

Algorithm 2 ULB-CPC with accuracy refinement

Input: $\epsilon_{\rm des}, N_{\max}$
Output: $\hat{p}_{\rm c}, \epsilon$
1: $N = 20$
2: $[\hat{p}_{\rm c}, \epsilon, \epsilon_{\max}] =$ ULB-CPC(N)
3: **while** $\epsilon_{\max} > \epsilon_{\rm des}$ and $N < N_{\max}$ **do**
4: $\quad N \leftarrow N + 10$
5: $\quad [\hat{p}_{\rm c}, \epsilon, \epsilon_{\max}] =$ ULB-CPC(N)
6: **end while**

The numerical results presented in this paper refer to the following set-up. The number of blocks is set to 50 for the MB-CPC method. The desired accuracy $\epsilon_{\rm des}$ is set to 0.005 for the MR-CPC and ULB-CPC methods. Finally, $D_{\max}$ and $N_{\max}$ are set to 20 and 200 in Algorithm 1 and Algorithm 2, respectively.

A. Description of the considered scenarios

Figure 2 represents the nominal and Monte Carlo realizations of two aircraft in the considered scenarios 1 and 2. Velocity of aircraft is set equal to 500 nmi/h in both scenarios. The origin and destination of the aircraft are given in Table I.

TABLE I: Origin and destination of the aircraft

Scenario No.	Aircraft No.	$\mathbf{r}^\top = [x\,(\text{nmi})\ y\,(\text{nmi})]$	
		Origin	Destination
1	1	[1.0 76.0]	[101.0 76.0]
	2	[271.0 76.0]	[13.0 76.0]
2	1	[41.0 86.0]	[251.0 86.0]
	2	[121.0 12.5]	[121.0 87.5]

B. Conflict probability estimation

Figures 3 show the inner and outer block covers of the conflict zone for scenario 1 and 2. The space partitions refer to $t = 1000$ and $t = 540$ seconds and are obtained with the MR-CPC method in scenario 1 and 2, respectively. As expected, the blocks that are far from the mean value $\Delta\bar{\mathbf{r}}$ of the relative aircraft distance (reported in the new (ξ, η) coordinates) are not divided, whereas those that are closer are divided into smaller ones.

Figure 4 plots the conflict probability obtained by the I-CPC, MB-CPC, ULB-CPC, and MR-CPC in scenarios 1 and 2. As for the I-CPC estimate, it provides an upper bound on the probability of conflict and it can hence deviate from the

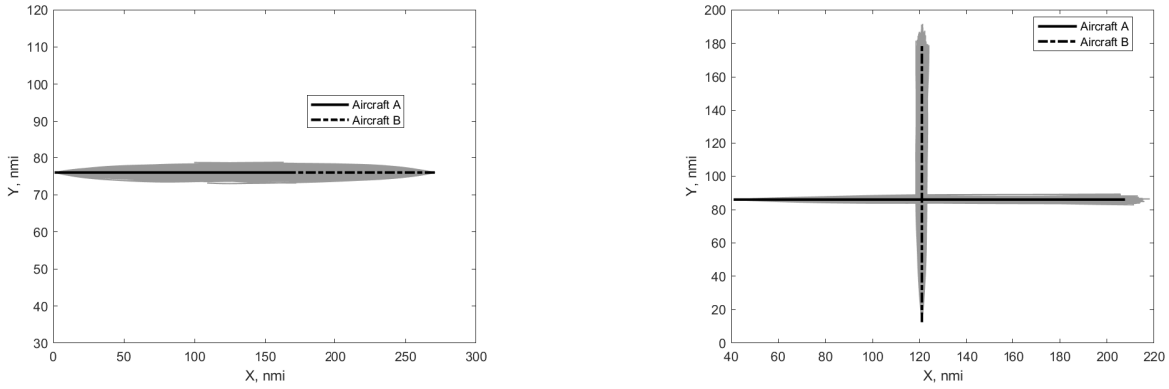

(a) (b)

Fig. 2: Nominal aircraft trajectories and Monte Carlo realizations: a) Scenario 1, b) Scenario 2

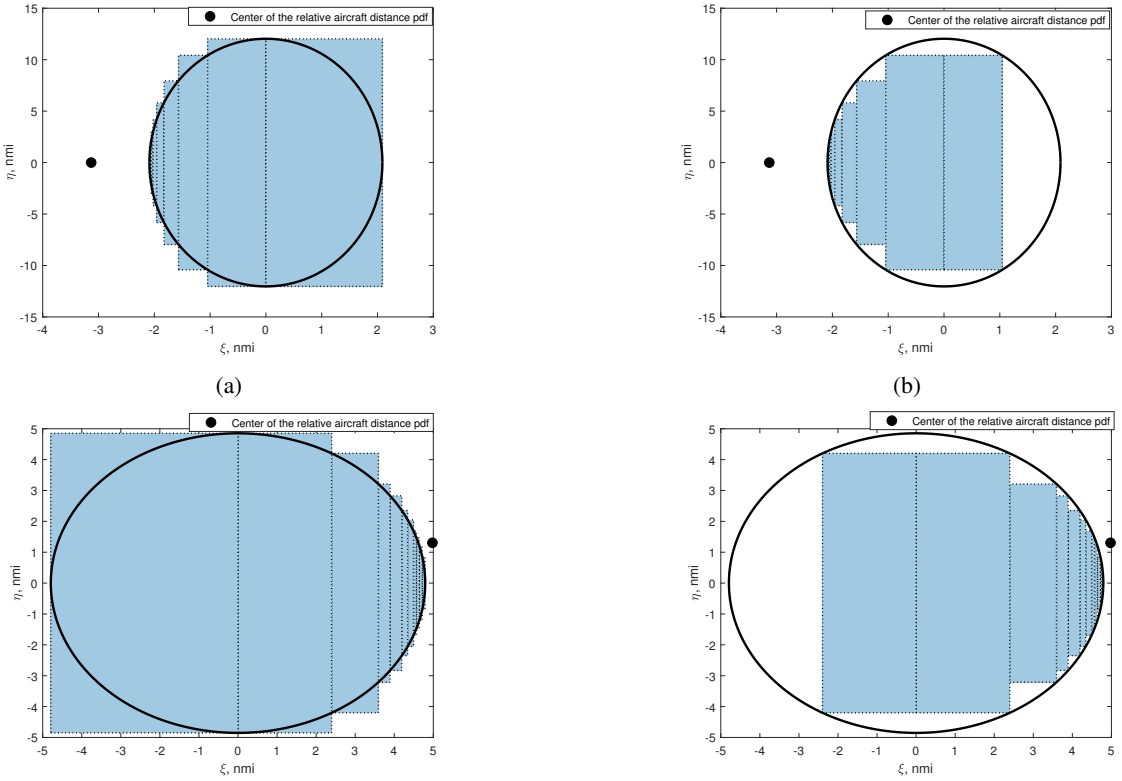

(a) (b)

(c) (d)

Fig. 3: Scenario 1: a) outer cover and b) inner cover of the conflict zone; Scenario 2: c) outer cover and d) inner cover of the conflict zone

values computed via Monte Carlo simulations as shown in Figure 4b. As for the MB-CPC, ULB-CPC, and MR-CPC methods, from Figure 4 it can be noted that they provide very close, basically identical estimates. The conflict probability estimates of the MB-CPC, ULB-CPC, and MR-CPC methods are close to the conflict probability p_c determined via Monte Carlo simulations. This is not surprisingly since the aircraft relative distance covariance matrix computed via Monte Carlo simulations is adopted.

Table II presents the computation time of the ULB-CPC and MR-CPC methods measured in a Matlab environment using a personal notebook with Intel core i7 processor and with 8 GB ram capacity. As the estimate of I-CPC and MB-CPC methods cannot be automatically refined, their computation time are not reported in Table II. Notably, the MR-CPC method proposed in this paper provides a more efficient block coverage of the conflict zone than the ULB-CPC method, with a smaller number of blocks needed to reach the same accuracy level. Therefore, MR-CPC requires less computation time compared to the ULB-CPC method.

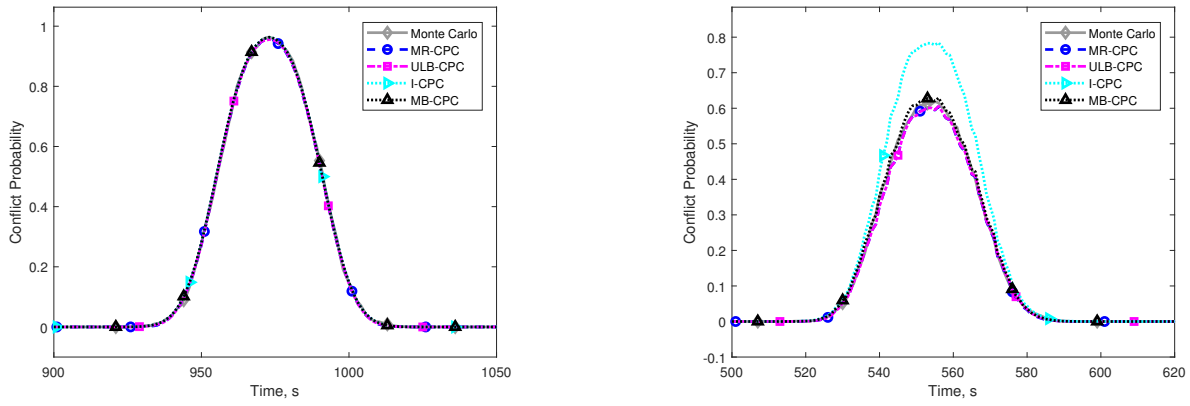

Fig. 4: Conflict probability estimation during the 2-aircraft encounter: a) Scenario 1, b) Scenario 2

TABLE II: Computation time of 100 runs

Scenario No.	t (s)	
	ULB-CPC	MR-CPC
1	29.7	21.2
2	21.4	20.6

VII. CONCLUSIONS

In this paper, we proposed a new method for aircraft conflict probability estimation, which uses an innovative spatial multi-resolution scheme when building the outer and inner block covers of the conflict zone adopted for conflict probability estimation.

The block covers are automatically tuned to the underlying probability distribution of the aircraft relative distance, which results in less computation time with respect to competitive methods when requiring the same accuracy level in the conflict probability estimation.

The method is introduced with reference to level flight. Further work is needed to extend it to a three-dimensional airspace setting.

REFERENCES

[1] "European aviation in 2040, challenges of growth, annex1," *EUROCONTROL*, 2018.

[2] R. Schaufele Jr, J. Corning, L. Ding, *et al.*, "Faa aerospace forecast: Fiscal years 2018-2038," *Washington, DC*, 2018.

[3] J. M. Hoekstra, R. N. van Gent, and R. C. Ruigrok, "Designing for safety: the 'free flight'air traffic management concept," *Reliability Engineering & System Safety*, vol. 75, no. 2, pp. 215–232, 2002.

[4] J. K. Kuchar and L. C. Yang, "A review of conflict detection and resolution modeling methods," *IEEE Transactions on Intelligent Transportation Systems*, vol. 1, no. 4, pp. 179–189, 2000.

[5] S. Seyedipour, H. Nobahari, and M. Prandini, "Probability estimation in aircraft conflict detection: a simple and computationally effective method with accuracy certificates," in *2019 18th European Control Conference (ECC)*. IEEE, 2019, pp. 4319–4324.

[6] G. Chaloulos and J. Lygeros, "Effect of wind correlation on aircraft conflict probability," *Journal of Guidance, Control, and Dynamics*, vol. 30, no. 6, pp. 1742–1752, 2007.

[7] I. Lymperopoulos and J. Lygeros, "Sequential Monte Carlo methods for multi-aircraft trajectory prediction in air traffic management," *International Journal of Adaptive Control and Signal Processing*, vol. 24, no. 10, pp. 830–849, 2010.

[8] M. Prandini, J. Lygeros, A. Nilim, and S. Sastry, "Randomized algorithms for probabilistic aircraft conflict detection," in *Proceedings of the 38th IEEE Conference on Decision and Control (Cat. No. 99CH36304)*, vol. 3. IEEE, 1999, pp. 2444–2449.

[9] M. Prandini, J. Hu, J. Lygeros, and S. Sastry, "A probabilistic approach to aircraft conflict detection," *IEEE Transactions on Intelligent Transportation Systems*, vol. 1, no. 4, pp. 199–220, 2000.

[10] Y. Yang, J. Zhang, K.-Q. Cai, and M. Prandini, "Multi-aircraft conflict detection and resolution based on probabilistic reach sets," *IEEE Transactions on Control Systems Technology*, vol. 25, no. 1, pp. 309–316, 2017.

[11] W. Liu, C. Seah, and I. Hwang, "Aircraft 4D trajectory prediction and conflict detection for air traffic control," *Proc. 49th Confer-ence on Decision and Control*, 2010.

[12] W. Liu and I. Hwang, "Probabilistic trajectory prediction and conflict detection for air traffic control," *Journal of Guidance, Control, and Dynamics*, vol. 34, no. 6, pp. 1779–1789, 2011.

[13] E. Hernandez-Romero, A. Valenzuela, and D. Rivas, "A probabilistic approach to measure aircraft conflict severity considering wind forecast uncertainty," *Aerospace Science and Technology*, vol. 86, pp. 401–414, 2019.

[14] E. Hernández-Romero, A. Valenzuela, and D. Rivas, "Probabilistic multi-aircraft conflict detection and resolution considering wind forecast uncertainty," *Aerospace Science and Technology*, vol. 105, p. 105973, 2020.

[15] T. Jones, "Tractable conflict risk accumulation in quadratic space for autonomous vehicles," *Journal of Guidance, Control, and Dynamics*, vol. 29, no. 1, pp. 39–48, 2006.

[16] C. E. Van Daalen and T. Jones, "Fast conflict detection using probability flow," *Automatica*, vol. 45, no. 8, pp. 1903–1909, 2009.

[17] J. Park and J. Kim, "Predictive evaluation of ship collision risk using the concept of probability flow," *IEEE Journal of Oceanic Engineering*, vol. 42, no. 4, pp. 836–845, 2017.

[18] R. A. Paielli and H. Erzberger, "Conflict probability estimation for free flight," *Journal of Guidance, Control, and Dynamics*, vol. 20, no. 3, pp. 588–596, 1997.

[19] I. Hwang and C. E. Seah, "Intent-based probabilistic conflict detection for the next generation air transportation system," *Proceedings of the IEEE*, vol. 96, no. 12, pp. 2040–2059, 2008.

[20] K.-Y. Baek and H.-C. Bang, "ADS-B based trajectory prediction and conflict detection for air traffic management," *International Journal of Aeronautical and Space Sciences*, vol. 13, no. 3, pp. 377–385, 2012.

[21] L. J. Pienaar and T. Jones, "The application of probability flow for conflict detection near airports," in *AIAA Guidance, Navigation, and Control Conference*, 2015, p. 1325.

[22] I. Lymperopoulos, "Sequential Monte Carlo methods in air traffic management," Ph.D. dissertation, ETH Zurich, 2010.

[23] I. Lymperopoulos, J. Lygeros, V. Lecchini Andrea, J. Maciejowski, and W. Glover, "A stochastic hybrid model for air traffic management processes," Cambridge University, Tech. Rep., 2007.

[24] M. Ballin and H. Erzberger, "An analysis of landing rates and separations at Dallas/Ft. Worth Airport," NASA Technical Memorandum, TM 110397, Tech. Rep., July 1996.

[25] C. Y. Young, *Precalculus*, 2nd ed. John Wiley & Sons, 2013.